IEEE Access
Multidisciplinary | Rapid Review | Open Access Journal

Received July 17, 2019, accepted July 30, 2019, date of publication August 12, 2019, date of current version August 27, 2019.

Digital Object Identifier 10.1109/ACCESS.2019.2934751

PCS Threshold Selection for Spatial Reuse in High Density CSMA/CA MIMO Wireless Networks

PHILLIP B. ONI, (Student Member, IEEE), AND STEVEN D. BLOSTEIN, (Senior Member, IEEE)
Department of Electrical and Computer Engineering, Queen's University, Kingston, ON K7L 3N6, Canada

Corresponding author: Phillip B. Oni (phillip.oni@queensu.ca)

This work was supported by the Natural Sciences and Engineering Research Council of Canada Discovery Grant 06237-2019.

ABSTRACT Multiple-input multiple-out (MIMO) equipment improves the spectral efficiency of wireless local area network (WLAN) systems. However, in a large-scale or dense MIMO WLANs, overlapping radio cells or basic service sets (BSSs) are inherent. This prevents multiple concurrent transmissions and degrades spatial reuse. The inability to separate multiple simultaneous transmissions in space is detrimental to overall system performance. The carrier sense multiple access collision avoidance (CSMA/CA) protocol uses the physical carrier sensing (PCS) threshold to determine channel state at the physical layer (PHY) and decide on the number of concurrent transmissions allowed per time slot. Since the PCS threshold determines the spatial reuse under the CSMA/CA protocol, which consequently determines the interference level and the network aggregate throughput, we address PCS threshold selection for dense uplink (UL) MIMO WLAN systems. A closed-form expression is derived for selecting the PCS threshold based on the fundamental parameters of the network where nodes are randomly placed according to a Poisson point process (PPP). We obtain the PCS threshold value that maximizes the *spatial density of throughput* (SDT) and study the effectiveness of the proposed framework under moderate to high node density. In addition, we analyze the effect of WLAN density on interference from concurrent transmitters. The key observation is that PCS threshold selection should take into account key network characteristics including node density, target SINR or threshold, path-loss exponent and antenna configuration.

INDEX TERMS Dense WLANs, node density, PCS threshold, dynamic sensitivity control, CSMA/CA, hidden terminal, exposed terminal, spatial reuse, successful transmission probability, physical carrier sensing.

I. INTRODUCTION

The increasing number of powerful mobile devices as well as the Internet of Things (IoT) is generating high aggregate data rates. This leads to the deployment of high-density wireless local area network (WLAN) access points (APs) in hotels, airports, enterprises, residential buildings, stadiums, cafés etc. to provide reliable wireless connectivity to densely distributed mobile users. This trend is expected to continue beyond the fifth generation (B5G) as devices proliferate combined with throughput-intensive applications that rely on the WLAN's carrier sense multiple access (CSMA) protocol for data services. As the density of nodes or devices per network area continue to increase, it becomes difficult to separate multiple concurrent transmissions in the network. In particular, in such large-scale WLANs (or IEEE 802.11 networks), spatial reuse and interference are the two major issues that hinder network performance and efficient content delivery [1], [2]. To address these issues, efficient physical carrier sensing (PCS) is paramount within the IEEE 802.11ax task group [3], [4] in the form of dynamic sensitivity control (DSC).

In IEEE 802.11 wireless networks, access to the medium is controlled through the distributed coordination function (DCF) access mechanism at the medium access control (MAC) layer. The DCF uses the (CSMA) with collision avoidance (CSMA/CA) protocol to govern contention among nodes and control access to the channel. Under the CSMA/CA protocol, nodes having packets to transmit are required to first sense the medium for ongoing or active transmissions. The sensing node measures the energy level on the channel within the carrier sensing range (CSR)[1] and

The associate editor coordinating the review of this article and approving it for publication was Yeon-Ho Chung.

[1] A range within which a node can detect an active transmission. This range depends on the selected PCS threshold and it determines the degree of spatial reuse.

compares the measured energy to a threshold known as the physical carrier sensing (PCS) threshold[2] to determine if the channel is *idle* or *busy*. A node can start transmitting its packet over an idle channel while a *busy* channel requires the node to defer its transmission. In current WLAN systems, the PCS threshold is static and not optimized for different network topologies or densities [1], [5]. The inefficiency of the static PCS threshold is currently being addressed to improve spatial reuse for next generation WLAN systems [6], as well as address performance degradation due to densification [7]. While a high PCS threshold value (low sensitivity) implies high interference as more concurrent transmissions are permitted, a low PCS threshold (high sensitivity) degrades spectral efficiency due to inefficient spatial reuse.

Managing spatial reuse effectively enables multiple simultaneous *successful* transmissions. The conventional CSMA/CA protocol with a fixed PCS threshold is often inefficient in achieving spatial reuse and suffers from two inherent problems that degrade performance [1]: the *hidden terminal* and the *exposed terminal*. The hidden terminal is any node outside of the CSR that initiates transmission during the transmission to the desired node, thereby causing a collision at the receiver. A node is said to be an exposed node when it defers its transmission because it is within the CSR when its transmission would otherwise be successful at the receiver. Careful PCS threshold selection is paramount to mitigating the effects of exposed and hidden terminal problems, and achieves increased aggregate throughput. With the recent introduction of long term evolution (LTE) system transmission within the unlicensed band, 802.11-based WLAN faces performance degradation without modification of the current CSMA/CA protocol [10].

For efficient spatial reuse and network-wide performance enhancement, nodes in a basic service set (BSS) or cell should not unnecessarily defer potential successful transmissions when nodes in neighboring BSSs are transmitting. This is motivated by the fact that as the density of nodes increases, it becomes difficult to separate simultaneous transmissions, and consequently, throughput degrades due to frequent backoffs, collisions, short spatial reuse and increased interference. Since the density of future IEEE 802.11 wireless networks are expected to grow and 802.11ax standardization aims to enhance the capacity of high density WLANs, it is paramount to seek an optimal PCS threshold that maximizes the aggregate system throughput or performance.

A. PROBLEM: PCS THRESHOLD SELECTION

To motivate the PCS threshold selection problem for high-density WLANs, consider Figure 1 where two user stations (STAs), STA_1 and STA_2 are associated with AP_2 and AP_1, respectively. Assume that both STAs have packets in their buffers at the same time-slot and the PCS threshold for carrier sensing (PCS) is Υ_1. STA_2 performs the PCS and discovers

[2]Sometimes referred to as the clear channel assessment (CCA) threshold in the literature.

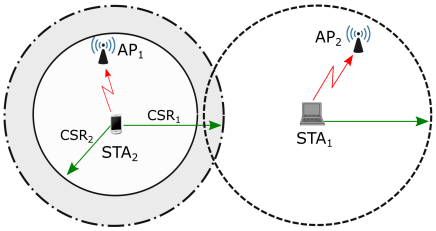

FIGURE 1. Physical carrier sensing range and threshold in the uplink.

that STA_1 is within its carrier sensing range CSR_1, and vice versa. Either STA_1 or STA_2 has to *backoff* for each other even though their respective transmissions will be successful at the APs. This unnecessary *back-off* occurs more frequently in *high density* networks where there are multiple overlapping CSRs or BSSs. For example, in a second scenario with Υ_2 as the PCS threshold, the CSR of STA_2 shrinks and no other transmission is detected within the CSR_2. In that case, STA_2 and STA_1 can transmit simultaneously, increasing the aggregate throughput. Hence, PCS threshold selection needs to be optimized with respect to throughput maximization objective. Thus, the fundamental question is *how do we select the PCS threshold* Υ *to improve throughput taking interference into account?* Some of the existing works addressing this problem are discussed subsequently.

B. EXISTING RELATED WORK

In current systems, the PCS threshold is static and often vendor dependent, and is not adaptive to network topologies, fading characteristics, path-loss and other conditions of the wireless network environment. Due to the inevitable increase in network density, wireless networks are becoming increasingly interference-limited, and the ineffectiveness of this static PC threshold selection has long been a subject of investigation [1] (see the references therein). The scale of today's wireless LANs requires adaptive selection of the PCS threshold for the specific network environment where the nodes will operate. Recent approaches mostly assume uniform distribution of nodes, uniform data rates, and single antenna [1]. The reality, however, is that a PCS threshold depends on random node distribution, channel fading characteristics, antenna configuration, path loss, node density. In [13], it is shown that PCS threshold adaptation enhances WLAN capacity. More precisely, adapting a PCS threshold such that the minimum SINR is maintained could yield significant improvement in throughput [6], [7].

As the density of today's WLANs continue to grow, improving spatial reuse becomes critical. The study in [6] provides performance analysis of existing PCS threshold and power control algorithms to determine if sensing threshold adaptation is worth implementing in future high density WLANs. For new generations of WiFi clients, PCS threshold adaptation that maintains minimum required SINR could improve performance in high density WLANs [6]. Recent research into improving the performance of large-scale

CSMA networks includes new channel access algorithms [7], CSMA-based protocol designs [8], [14]–[16], dynamic tuning of the PCS threshold [3], [4], [17]–[26] and optimization of the PCS threshold to maximize performance [5], [12], [27]–[29]. Using Basic Service Set (BSS) coloring information and considering minimum SINR level in [7], an algorithm is proposed to dynamically adjust transmit power and channel access rules in WLANs. This approach requires perfect interference estimation at the receiver to achieve minimum SINR.

In the same vein, an enhanced variant of the listen-before-talk (LBT) or CSMA/CA protocol is proposed in [14] to facilitate efficient frequency reuse and interference avoidance when licensed-assisted access (LAA) for LTE systems coexists with 802.11 networks in the unlicensed band. The enhanced LBT schemes incorporate PCS threshold adaptation to avoid interference and increase channel access opportunity. An adaptive channel access scheme is proposed in [16] that exploits the information-theoretic capacity region of a multiple access channel. Exploiting the capacity region to determine the channel access strategy of a node, appears similar to opportunistic CSMA [8], [15] where nodes with good channels are allowed to contest for channel access while neglecting to properly choose the PCS threshold, which determines spatial reuse.

Under the 802.11ax working group, dynamic sensitivity control (DSC) [3], [4], [17]–[26] is recommended as an alternative scheme to the conventional static PCS threshold. The PCS threshold for DSC is implemented by setting a minimum (default sensitivity) and a maximum permissible, usually between -82 and -30 dBm [4], [17], [18], [20] and the PCS threshold is chosen from this range based on transmission loss rate [4], [25], achievable throughput [17], [20], collision rate [18] and the measured received signal strength indicator (RSSI) between the target AP and its neighbor [20]. Since the performance of DSC over the PCS threshold varies from one topology and node density to another [3], it is important to select the PCS threshold margin for DSC based on specific network characteristics such as path loss, node density and fading. The protective clear channel assessment (ProCCA) [23] and fine-grained adaptation of carrier sensing threshold (FACT) [24] aim to improve spatial reuse by setting the PCS threshold according to the network information contained in the PHY header including measured interference.

Similar to [23], [24], using measured network information, [21] and [22] propose a DSC for IEEE 802.11ax APs to dynamically adjust the PCS threshold of an AP based on received signal strength (RSS) from its associated stations and interfering APs. New schemes to configure the PCS threshold based on signal-to-interference-and-noise ratio (SINR) in dense CSMA networks are proposed in [34]. To ensure interference-free transmissions, a static approach to set a global PCS threshold and a dynamic adjustment scheme based on the feedback of nearby transmissions, are proposed. Using the properties of stochastic geometry [27]–[31], a PCS threshold selection rule (DSC scheme) that accounts for the randomness of user location or node distribution and the channel access behavior, is investigated. Assuming stations (STAs) and APs are distributed according to independent homogeneous Poisson point process (PPP) [27], [28], the PCS threshold can be configured for *cell-edge* STAs by examining the information (link quality, average RSSI from neighbors) in *beacon* frames [27] and provide performance analysis of the DSC scheme given a range of PCS threshold values [28]. For a PPP network, the impact of the CSR on link performance is analyzed in [29], [30] to obtain a bound on the CSR and that bound is used to perform PCS threshold adjustment in a way similar to that of the DSC approaches.

Likewise, [31] provides an analysis of the DSC scheme for Poisson-distributed networks where a default PCS threshold and fixed threshold to update the PCS threshold are known *a priori*. Joint optimization of the PCS threshold and transmission rate for single-input single-out (SISO) Poisson ad hoc networks appears in [32]. Similar to [32], an analytical solution for optimal PCS threshold reveals the relationship between network capacity, PCS threshold and transmit power, and offers a technique to derive the CSR as a function of node density, access probability and duration of each channel state [33]. A host of proposed DSC schemes [4], [17]–[20], [25] are based on *probing* procedures where nodes select PCS threshold values from a range of values depending on observed or measured network information. This measurement-based scheme could degenerate spectral efficiency over time as the system needs to keep track of changes in the network to update the PCS threshold. Also, improper PCS threshold margin could jeopardize the advantages of DSC as a result of collisions and disparity in the degree of fairness in accessing the channel [3]. Efficient implementation of DSC schemes requires an adequate range of threshold values, and there is no consensus on a rule for their selection.

In summary, none of the previous approaches to uplink PCS [1], [4]–[34] exploits the multi-antenna nature of current WLANs. Also, the DSC schemes, ProCCA and FACT [4], [17], [26] require extensive channel measurement overhead. Adapting the PCS threshold based on this measured network information is further complicated by the CSMA/CA protocol, especially in high-density networks and may not guarantee optimality. The enhanced CSMA protocols proposed and analyzed so far [8], [15], [16] require knowledge of the optimal PCS threshold to guarantee optimal spatial reuse but do not propose methods for PCS threshold optimization. Finally, the PCS threshold should be optimized to prevent the hidden terminal and the exposed terminal problems inherent in the CSMA/CA protocol [1], [5], which are not addressed by the existing schemes [4], [8]–[34]. Finally, optimizing the PCS threshold based on prior network information is more practical in large-scale WLAN as it avoids costs associated with persistent network monitoring.

In this paper, by considering the underlying PHY layer characteristics of the carrier sensing process, we address PCS threshold selection differently by jointly considering density

of nodes, multi-antenna configuration, channel fading and path loss. Herein, the performance metric of interest is the *spatial density of throughput* (SDT), which is the average number of successful transmission per unit area [9], [10]. We seek to maximize the SDT by optimizing the PCS threshold for an arbitrary density of nodes, path loss exponent and assuming multi-antenna nodes i.e., multiple-input multiple-output (MIMO) with channel gains characterized by a *one-ring* scattering model [38]. In terms of fairness, it is assumed that all nodes contend for the channel with equal probability.

To consider the hidden and the exposed terminal problems, two constraints are introduced into the optimization problem to account for their effects in PCS threshold selection. This is important because the existence of hidden terminals results in collisions at the receiver, causing persistent retransmissions while exposed terminals could depress spatial reuse. The tradeoff is that a high PCS threshold allows for the existence of *hidden nodes* while a low PCS threshold creates *exposed nodes*. Hence, the fundamental question is *how do we optimize the PCS threshold* Υ *to achieve a balance in the trade off between the hidden terminal problem and the exposed terminal problem?* The proposed PCS threshold selection method is compared to the legacy scheme and the DSC scheme [41] as applied by [28] for stochastic networks. In addition to optimizing the PCS threshold, we determine the maximum density of nodes (densification) that yields improved performance.

C. CONTRIBUTIONS AND ORGANIZATION

In recent prior work [12], the impact of optimizing the PCS threshold to maximize the density of throughput is addressed for SISO wireless networks. In this contribution, we extend our investigation to MIMO wireless networks taking into account the trade-off between hidden and exposed terminal problems. The contributions are highlighted as follows:

- Using tools from stochastic geometry, specifically the PPP, to model the randomness of node locations and traffic in high-density networks, we formulate a throughput maximization problem to mitigate the inherent hidden terminal and the exposed terminal problems in high density WLAN by optimizing the PCS threshold. Given antenna configuration (MIMO), path loss, node density and fading characteristics of the wireless environment, we maximize the spatial density of throughput (SDT).
- We derive a closed-form mathematical expression for selecting the PCS threshold. The proposed PCS threshold selection scheme avoids frequent channel sounding and network measurement but requires knowledge of node density, path loss exponent, and antenna configuration that are usually known a priori. For a performance benchmark, we simulate the proposed PCS threshold selection method under the DCF CSMA/CA protocol. The performance of the proposed scheme is compared to that of the legacy system and the DSC scheme [41].

The remaining parts of this paper are organized as follows: the system model and assumptions are presented in Section II. In Section III, we derive a node's channel access probability based on the CSMA/CA protocol, the successful transmission probability and present the performance metric. The proposed PCS threshold selection framework is presented in Section IV while its performance is discussed in Section V. Section VI provides the main conclusions.

D. NOTATION

The following notations are used throughout this paper. Boldface uppercase letters represent matrices. For instance, matrix $\mathbf{H}$ represents the channel matrix between a user and an AP. Column vectors are denoted as boldface lowercase letters such as $\mathbf{x}$ representing the transmitted symbols. The expected value of any random variable will be denoted as $\mathbb{E}[\cdot]$. The Frobenius norm of a matrix is denoted as $\|\cdot\|^2$. Superscripts $[\cdot]^H$ and $[\cdot]^T$ represent Hermitian (conjugate transpose) and transpose, respectively.

II. SYSTEM AND NETWORK MODEL

A. NETWORK MODEL AND ASSUMPTIONS

We consider a WLAN where STA and AP locations are modeled as independent homogeneous Poisson point processes (PPPs) with respective intensities, λ_n and λ_m. This choice is motivated by the fact that PPPs are suitable for modeling dense networks [35] and STAs/APs are not usually deployed in a regular grid due to physical constraints. Let $\mathcal{N}$ represent the set representing the PPP of STAs and $\mathcal{A}$ represent the set of APs in the network. Subsequently, we focus primarily on deriving the performance metric and the optimal PCS threshold for uplink (UL) transmissions. This is due to the fact that contention in the UL is usually more severe than that of the downlink (DL), since in most WLANs, there are more user STAs than APs. For example, in Internet of Things (IoT) applications, the UL may be the bottleneck because large numbers of devices that sense the environment need to transmit their information to a central AP. In this sensing scenario, much less information would flow in the DL direction. Throughout this paper, based on Assumption 1, we focus primarily on optimizing the PCS threshold selection for the UL:

Assumption 1: While STAs are randomly located in the network, APs are well planned and deployed in such a pattern that allows sufficient separation of multiple concurrent downlink transmissions in space. In other words, adequate CSR is achieved through proper planning of AP deployment, which is achieved through spacing of APs in the network.

B. MIMO CHANNEL MODEL AND ASSUMPTION

Figure 2 depicts an uplink channel or multiple access channel (MAC) of an STA. The STA is equipped with U_t transmit antennas while the AP receiver has a sectorized linear K_r-element antenna array. For a typical n^{th} STA $n = 1, \ldots, |\mathcal{N}|$ the U_t transmitted signals are modeled as random

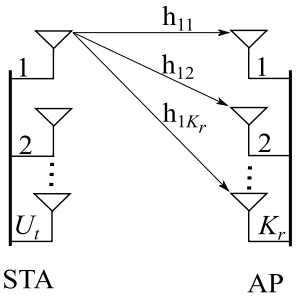

FIGURE 2. Uplink MIMO channel model between one STA and and its associated AP.

variables $x_1, \ldots x_{U_t}$ and the signal vector is denoted as $\mathbf{x}_n \in \mathbb{C}^{U_t \times 1} = \left[x_1, x_2, \ldots x_{U_t}\right]^T$. The pre-processing received signal $\mathbf{y} \in \mathbb{C}^{K_r \times 1}$ at the AP is:

$$\mathbf{y} = \underbrace{\mathbf{H}_n \mathbf{x}_n}_{\text{desired signal}} + \underbrace{\sum_{\kappa \in \mathcal{K}, \kappa \neq n | \mathcal{K} \subset \mathcal{N}} \mathbf{H}_\kappa \mathbf{x}_\kappa}_{\text{co-channel interference}} + \underbrace{\mathbf{n}_o}_{\text{effective noise}}, \tag{1}$$

where $\mathbf{H}_n$ is the $K_r \times U_t$ UL channel coefficient matrix between STA$_n$ and the AP whose entries are circularly symmetric complex Gaussian random variables with zero-mean and unit variance. In (1), $\mathbf{H}_\kappa \in \mathbb{C}^{K_r \times U_t}$ represents the channels of concurrent transmitting STAs, κ, other than STA n whose signals are received at the AP as interference and $\mathbf{n}_o$ is the $K_r \times 1$ independent and identically distributed (i.i.d) Gaussian noise vector with zero-mean and variance $\sigma^2_{n_o}$.

Therefore, in the presence of interference from $\mathcal{K}$ other STAs (concurrent transmitters), the post-processing signal-to-interference-plus noise (SINR) of STA$_n$ at the AP is written as follows:

$$\begin{aligned} \text{SINR}_n &= \frac{\mathbb{E}\left[\left|\mathbf{W}_n \mathbf{H}_n \mathbf{x}_n\right|^2\right]}{\mathbb{E}\left[\left|\sum_{\kappa \in \mathcal{K}, \kappa \neq n | \mathcal{K} \subset \mathcal{N}} \mathbf{W}_n \mathbf{H}_\kappa \mathbf{x}_\kappa + \mathbf{W}_n \mathbf{n}_o\right|^2\right]} \\ &= \frac{\left|\mathbf{W}_n^H \Theta_n \mathbf{R}_n \mathbf{W}_n\right|^2}{\left|\sum_{\kappa \in \mathcal{K}, \kappa \neq n | \mathcal{K} \subset \mathcal{N}} \mathbf{R}_{\mathbf{H}_\kappa \mathbf{x}_\kappa + \mathbf{n}_o}\right|^2}, \end{aligned} \tag{2}$$

where $\mathbf{R}_n = \mathbb{E}\left[\mathbf{H}_n \mathbf{H}_n^H\right]$, $\mathbf{W}_n = \left(\mathbf{H}_n^H \mathbf{H}_n\right)^{-1} \mathbf{H}_n^H$ is the $U_t \times K_r$ receiver beamformer matrix whose column vectors $\mathbf{w}_1, \mathbf{w}_2, \ldots, \mathbf{w}_{K_r}$ represent the block of linear filters at the AP, given symbol energy $\mathcal{E}_x$, for a signal angle of arrival θ_n, the zero mean transmitted signal correlation matrix $\Theta_n = \mathbb{E}\left[\mathbf{x}_n \mathbf{x}_n^H\right] = e^{j2\theta_n} U_t \mathcal{E}_x \mathbf{I}_{U_t}$, and $\mathbf{R}_{\mathbf{H}_\kappa \mathbf{x} + \mathbf{n}_o}$ is the correlation matrix of the interference-plus-noise at the AP expressed as:

$$\begin{aligned} &\mathbf{R}_{\mathbf{H}_\kappa \mathbf{x}_\kappa + \mathbf{n}_o} \\ &= \mathbb{E}\left[\left(\mathbf{W}_n^H \mathbf{H}_\kappa \mathbf{x}_\kappa + \mathbf{n}_o \mathbf{W}_n\right)\left(\mathbf{W}_n^H \mathbf{H}_\kappa \mathbf{x}_\kappa + \mathbf{n}_o \mathbf{W}_n\right)^H\right]. \end{aligned} \tag{3}$$

By exploiting the fact that $\mathbb{E}\left[\mathbf{n}_o \mathbf{n}_o^H\right] = \sigma^2_{n_o} \mathbf{I}_{K_r}$ and assuming that the transmitted signals are uncorrelated, we have:

$$\begin{aligned} \mathbf{R}_{\mathbf{H}_\kappa \mathbf{x}_\kappa + \mathbf{n}_o} &= \mathbf{W}_n^H \left(\mathbf{H}_\kappa \Theta_\kappa \mathbf{H}_\kappa^H + \mathbb{E}\left[\mathbf{n}_o \mathbf{n}_o^H\right]\right) \mathbf{W}_n \\ &= \mathbf{W}_n^H \left(\mathbf{R}_\kappa \Theta_\kappa + \mathbb{E}\left[\mathbf{n}_o \mathbf{n}_o^H\right]\right) \mathbf{W}_n, \end{aligned} \tag{4}$$

where $\Theta_\kappa = \mathbb{E}\left[\mathbf{x}_\kappa \mathbf{x}_\kappa^H\right] = e^{j2\theta_\kappa} U_t \mathcal{E}_x \mathbf{I}_{U_t}$, $\mathbf{R}_\kappa = \mathbb{E}\left[\mathbf{H}_\kappa \mathbf{H}_\kappa^H\right]$ denotes the spatial correlation of the interference channel $\mathbf{H}_\kappa$ at the receiver AP and $\mathbb{E}\left[\mathbf{n}_o \mathbf{n}_o^H\right] = K_r \sigma^2_{n_o} \mathbf{I}_{K_r}$. To obtain an expression for the correlation matrices $\mathbf{R}_\kappa$ and $\mathbf{R}_n$, we employ

Assumption 2: To determine the spatial fading correlation of channels $\mathbf{H}_n$ and $\mathbf{H}_\kappa$, the one-ring scattering model (a geometry-based stochastic model) [38] is assumed, where without loss of generality, both the transmitter and the receiver have the same antenna element spacing.

The correlation matrix $\mathbf{R}_\kappa$ of the channel $\mathbf{H}_\kappa$ can be described based on a geometrical arrangement of the antenna elements at both the transmitter and the receiver. Under Assumption 2, the one-ring model represents a Rayleigh-fading channel where the single-bounce scatterers are located and dominant around the STA provided the AP is elevated and not affected by local scattering. Let R denote the radius of the scattering ring and θ_n denote the angle of arrival at the receiving AP. The angle of the incoming signal is within the range $[\theta_n - \Delta, \theta_n + \Delta]$ where $\Delta = \arcsin\left(\frac{R}{D}\right)$ is the angle spread of the scatterers. The interference channel correlation under the *one-ring* channel scattering model [38] is:

$$\mathbf{R}_\kappa = \mathbb{E}\left[\mathbf{H}_\kappa \mathbf{H}_\kappa^H\right] \tag{5}$$

$$\begin{aligned} &= \frac{1}{2\pi} \int_0^{2\pi} \exp\left\{-j\frac{2\pi}{\omega}\left[\psi_x\left(\left(1 - \frac{\Delta^2}{4} + \frac{\Delta^2 \cos 2\theta_n}{4}\right)\right.\right.\right. \\ &\quad \left.\left.\left. + \sin\theta_n\right) + \psi_y\left(\Delta \sin\theta_n + \cos\theta_n\right)\right]\right\} d\theta_n, \end{aligned} \tag{6}$$

where ω is the wavelength of the signal, ψ_x and ψ_y are antenna element spacings on the x-axis and the y-axis, respectively. For tractability, we further assume that the transmitting and the receiving antenna elements are aligned on the y-axis, which implies $\psi_x = 0$ in (6). Therefore,

$$\mathbf{R}_\kappa = \underbrace{\frac{1}{2\pi} \int_0^{2\pi} \exp\left\{-j\frac{2\pi}{\omega}\left[\psi_y\left(\Delta \sin\theta_n + \cos\theta_n\right)\right]\right\} d\theta_n}_{J_0(\cdot)}, \tag{7}$$

where $J_0(\cdot)$ is the Bessel function of the first kind of the zeroth order [36], [38]. The value of θ_n depends on the antenna geometry; for details, readers are referred to [38]. Later in Section III-C, $\mathbf{R}_\kappa$ is applied to derive the STP of a typical node, and it is shown that the STP (and consequently, PCS threshold selection) in our framework does not require channel sounding but only the knowledge of spatial geometry via θ_n.

III. PERFORMANCE METRIC

In this section, we introduce two important performance metrics that govern performance in WLANs, namely, the channel

access probability (CAP) and the successful transmission probability (STP). The CAP is the probability that a node gains access to the channel under the CSMA/CA protocol following a contention period. The STP (a.k.a the coverage probability [9] or transmission success probability [8]) measures the probability that a node achieves the target SINR to successfully decode the transmitted packets. Based on the CAP and STP, we next define the key performance metric, the spatial density of throughput (SDT) [9], [10], which quantifies the average number of users per unit area that *gain access to the medium* and *achieve the target SINR*.

A. CSMA/CA PROTOCOL MODEL

In conventional slotted CSMA wireless networks, nodes contend for the shared medium by sensing the channel. The CSMA/CA protocol utilizes physical carrier sensing (PCS) for channel contention. In PCS, a node with a packet in its buffer senses the channel within its carrier sensing range (CSR) and transmits in a time slot no other transmitting nodes are sensed. A packet is transmitted if the power sensed in the channel is below the PCS threshold Υ. A channel is flagged as idle if the power sensed within its CSR does not exceed the PCS threshold. In other words, the CSR represents a node's contention domain or neighborhood, and a node wins contention in its neighborhood if the power or energy sensed in the channel is below the PCS threshold.

To model the PCS process of the CSMA/CA protocol, let $\tilde{\mathcal{N}_c}$ denote the contention neighborhood of STA$_n$ and let $D_{n\tilde{n}}$ represent the distance between STA$_n$ and any other potential contending STA$_{\tilde{n}}$ within the contention domain. STA$_n$ in $\tilde{\mathcal{N}_c}$ will transmit if it senses an idle channel for the duration of the contention period. If the power is above the PCS threshold, it backs off by a random amount of time that is uniformly distributed. It transmits in the next time-slot where (i) it has the lowest backoff time in its neighborhood and (ii) the channel remains idle for the contention period. Therefore, at each time slot, a given STA$_n$ contends with other STAs in its neighborhood $\tilde{\mathcal{N}_c}$, given by

$$\tilde{\mathcal{N}_c} = \left\{ \tilde{n} \in \mathcal{N} \text{ s.t. } \|\mathbf{H}_{n\tilde{n}}\|^2 \; D_{n\tilde{n}}^{-\alpha} \Theta_{\tilde{n}} + \mathbb{E}\left[\|\mathbf{n}_o\|^2\right] > \Upsilon, n \neq \tilde{n} \right\}, \quad (8)$$

where the left-hand side of the inequality denotes the total power received by STA$_n$ from a neighboring STA$_{\tilde{n}}$ during carrier sensing, which is being checked against the PCS threshold Υ to determine an *idle* or *busy* channel. $\|\mathbf{H}_{n\tilde{n}}\|^2 = \text{Tr}\left(\mathbf{H}_{n\tilde{n}}\mathbf{H}_{n\tilde{n}}^H\right)$ represents the signal power received from a neighboring STA $\tilde{n}$ during carrier sensing, $D_{n\tilde{n}}$ is the spatial distance between STA$_n$ and its contending neighbor STA$_{\tilde{n}}$, α is the path loss exponent, and $\Theta_{\tilde{n}} = \left|e^{j2\theta_{\tilde{n}}} U_t \mathcal{E}_x \mathbf{I}_{U_t}\right|^2$. STA$_n$ is deemed to be in the contention neighborhood of STA$_{\tilde{n}}$, if STA$_{\tilde{n}}$ is located within the CSR of STA$_n$, i.e.,

$$\tilde{\mathcal{N}_c} = \left\{ \tilde{n} \in \mathcal{N} \text{ s.t. } D_{n\tilde{n}} \leq \chi, n \neq \tilde{n} \right\}, \quad (9)$$

where χ denotes the CSR of STA$_n$, which is determined based on the chosen PCS threshold. The neighborhood (or contention domain) in (9) is used next to derive the CAP of a node.

B. CHANNEL ACCESS PROBABILITY (CAP)

The CAP is the probability that STA$_n$ transmits, i.e., accesses the channel following contention. The density of concurrent transmitters permitted by the CSMA/CA protocol to transmit simultaneously per time slot depends on each user's CAP. The CAP is obtained according to

Lemma 1: STA$_n$ in neighborhood $\tilde{\mathcal{N}_c}$ gains access to the channel with probability

$$\mathcal{P}_n^c = 1 - \left[\lambda_n \Gamma\left(\frac{1}{\alpha}\right) \left(\frac{\Upsilon - \left|U_r \sigma^2 \mathbf{I}_{U_r}\right|^2}{\Theta_{\tilde{n}}} \right)^{-\frac{1}{\alpha}} \frac{1}{\alpha} \right], \quad (10)$$

where λ_n is the density of STAs defined in Section II-A, $\Gamma(\cdot)$ is the Gamma function, and U_r denotes the number of receiving antennas at the STA performing the PCS process. Eqn. (10) reveals that the CAP of a node depends on the path loss exponent α between the sensing node and its neighbors, the number of antennas used for sensing and the node density λ_n, which determines its contention neighborhood or domain.

Proof: When a packet arrives in STA$_n$'s buffer, it senses the channel for any active transmission in its neighborhood $\tilde{\mathcal{N}_c}$ defined according to (8), which represents the set of nodes whose signals could collide with STA n's signal if they transmit concurrently; that is, if the channel contains signal power above Υ. The CAP that STA n senses an idle channel is:

$$\begin{aligned}
\mathcal{P}_n^c &= 1 - \mathbb{P}\left(\|\mathbf{H}_{n\tilde{n}}\|^2 \cdot D_{n\tilde{n}}^{-\alpha} \Theta_{\tilde{n}} + \mathbb{E}\left[\|\mathbf{n}_o\|^2\right] > \Upsilon \right) \\
&= 1 - \mathbb{P}\left(\text{Tr}\left(\mathbf{H}_{n\tilde{n}}\mathbf{H}_{n\tilde{n}}^H\right) > \frac{\Upsilon - \mathbb{E}\left[\|\mathbf{n}_o\|^2\right]}{D_{n\tilde{n}}^{-\alpha}\Theta_{\tilde{n}}} \right) \\
&\overset{(a)}{=} 1 - \mathbb{E}_{\mathcal{N}_n}\left[\prod_{\tilde{n}} \exp\left(-\frac{\Upsilon - \mathbb{E}\left[\|\mathbf{n}_o\|^2\right]}{D_{n\tilde{n}}^{-\alpha}\Theta_{\tilde{n}}} \right) \right] \\
&\overset{(b)}{\geq} 1 - \exp\left(-\mathbb{E}_{\mathcal{N}_n}\left[\sum_{\tilde{n}\in\mathcal{N}_n} \frac{\Upsilon - \mathbb{E}\left[\|\mathbf{n}_o\|^2\right]}{D_{n\tilde{n}}^{-\alpha}\Theta_{\tilde{n}}} \right] \right) \\
&\overset{(c)}{=} 1 - \lambda_n \int_{\mathbb{R}^2} \exp\left(-\frac{\Upsilon - \mathbb{E}\left[\|\mathbf{n}_o\|^2\right]}{D_{n\tilde{n}}^{-\alpha}\Theta_{\tilde{n}}} \right) \text{d}\, D_{n\tilde{n}} \\
&\overset{(d)}{=} 1 - \left[\lambda_n \cdot \Gamma\left(\frac{1}{\alpha}\right) \cdot \left(\frac{\Upsilon - \left|U_r\sigma^2\mathbf{I}_{U_r}\right|^2}{\Theta_{\tilde{n}}} \right)^{-\frac{1}{\alpha}} \cdot \frac{1}{\alpha} \right], \quad (11)
\end{aligned}$$

where $\left|U_r\sigma^2\mathbf{I}_{U_r}\right|^2 = \mathbb{E}\left[\|\mathbf{n}_o\|^2\right]$ for U_r receive antennas at STA$_n$. In (11), (a) follows from the fact that $\text{Tr}\left(\mathbf{H}_{n\tilde{n}}\mathbf{H}_{n\tilde{n}}^H\right)$ is a sum of exponential random variables and has a Chi-Square distribution with $2U_r$ DoF, (b) holds from Jensen's inequality since is a convex function, (c) is obtained by Campbell's theorem, $\mathbb{E}\left(\sum_{x\in\Phi} f(x)\right) = \lambda \int_{\mathbb{R}^2} f(x)\text{d}x$, [37, Eqn. (4.10) p. 114] and (d) follows from applying [36, Eqn. (3.326.1)], which establishes Eqn. (10). ■

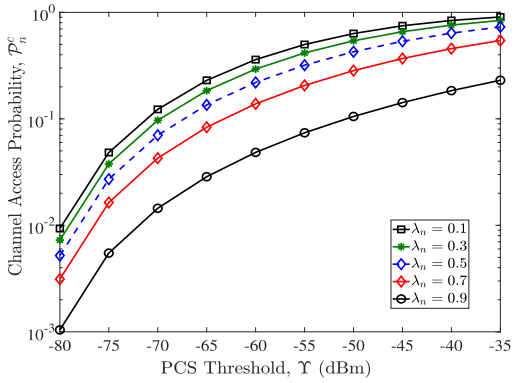

FIGURE 3. Channel access probability versus PCS thresholds for various node densities λ_n and $U_t = U_r = 1$.

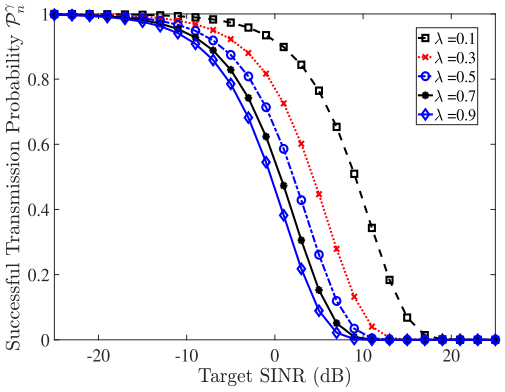

FIGURE 4. Successful transmission probability for various node densities and SINR thresholds given $K_r = 8$.

Figure 3(a) depicts the relationship between PCS threshold and channel access probability established in Lemma 1. At low PCS threshold, the CSR becomes larger and there are more nodes within the contention neighborhood of node. On the other hand, as the PCS threshold increases, the CSR of a typical node decreases and its probability of winning the channel contention increases. Without loss of generality, since channel state information (CSI) is not known at the STAs, it is assumed that the signal measured at one STA antenna output during PCS is used to measure interference *isotropically* to determine an "idle" or a "busy" channel.

C. SUCCESSFUL TRANSMISSION PROBABILITY (STP)

Gaining access to the channel does not guarantee a target SINR due to interference in large networks, especially in cases where STAs have high channel access probability (CAP); high CAP may cause high interference from densely distributed users, which causes erroneous decoding of transmitted symbols at the receiver AP. The probability of successful transmission in terms of achieving a specific data rate at a given SINR threshold is given in

Lemma 2: STA$_n$ achieves target SINR γ at the receiver AP with probability

$$\begin{aligned}\mathcal{P}_n^\gamma &= \mathbb{E}\left[\sum_{n\in\mathcal{N}} \mathbb{1}_{SINR_n>\gamma}\right] \\ &= \exp\left(-\gamma \left\|\mathbf{W}_n\right\|^2 \left|K_r \sigma_{n_o}^2 \mathbf{I}_{K_r}\right|^2\right) \\ &\quad \times \exp\left(-\gamma \left|\mathbf{W}_n^H \left(\left|e^{j2\theta_\kappa} U_t \mathcal{E}_x \mathbf{I}_{U_t}\right|^2 \lambda_n \left(\psi_y \frac{2\pi}{\omega}\right)^{-1} \right.\right.\right. \\ &\quad \left.\left.\left. e^{-\psi_y \frac{2\pi}{\omega}}\right) \mathbf{W}_n\right|^2\right), \quad (12)\end{aligned}$$

where ω is the wavelength of the channel carrier frequency and ψ_y is the antenna spacing aligned on the y-axis at both the transmitter and the receiver.

Proof: see Appendix A.

The probability of successful transmission for a particular node depends on the target rate in terms of the SINR threshold γ, the number of antennas at both the transmitters and the receiver, and ultimately the density of nodes that are generating interference through concurrent transmissions. Evaluating the transmission success probability derived from Lemma 2, Figure 4 provides insight. As expected, increasing the node density affects the receiver performance in terms of achieving the target SINR. At very low target SINR, for instance, -25 dB, the probability of successful transmission approaches 1 regardless of the node density. Here, the interference level is not an issue. However, increasing the node density increases the interference level due to the large number of concurrent transmitters. This demonstrates that it is imperative to find a tradeoff between increasing node density and achieving high SINR (or rate); this tradeoff can be captured in finding the optimal PCS threshold that maximizes a throughput objective. Since the PCS threshold determines the maximum number of concurrent transmitters per time slot, optimizing the PCS threshold reduces interference.

D. SPATIAL DENSITY OF THROUGHPUT (SDT)

The implication of multiple users with high CAPs is strong interference as many users will transmit concurrently causing strong interference and low SINRs. To capture the effect of interference and the CAP, SDT is defined as:

$$\mathcal{R}_{\text{SDT}} = \lambda_n \mathcal{P}_n^c \mathcal{P}_n^\gamma \quad (13)$$

where $\mathcal{P}_n^c$ is the probability that STA$_n$ gains access to the channel at a given time slot through the PCS process, which is obtained in Lemma 1. $\mathcal{P}_n^\gamma$ is the probability that an STA achieves SINR above a threshold γ, for the receiving AP to successfully decode a packet and it is derived in Lemma 2. For a fixed system bandwidth B, the *mean rate* $\bar{\mathcal{R}}$ is:

$$\bar{\mathcal{R}} = (B \log(1+\gamma))\, \mathcal{R}_{\text{SDT}} \quad \text{nats/sec/Hz.} \quad (14)$$

IV. PROPOSED PCS THRESHOLD OPTIMIZATION

A. PROBLEM FORMULATION

In this section, we optimize the PCS threshold to maximize the SDT defined in Eqn. (13) and maximizing $\mathcal{R}_{\text{SDT}}$ also

maximizes the mean rate $\bar{\mathcal{R}}$ defined in (14). This problem is formulated as follows:

$$\begin{aligned} &\text{maximize} && \mathcal{R}_{\text{SDT}} && \text{(15a)}\\ &\text{subject to} && \mathbb{I}_c \leq \Upsilon, && \text{(15b)}\\ & && P_I \leq \beta, \quad \text{and} && \text{(15c)}\\ & && \Upsilon > 0, \quad \forall n \in \mathcal{N}, && \text{(15d)} \end{aligned}$$

where constraint (15b) represents the PCS threshold constraint that the total power $\mathbb{I}_c$ sensed by a node is below the PCS power threshold Υ. To account for inter-BSS interference, the interference power at the receiving AP is constrained by (15c) where β is the interference power threshold (minimum tolerable interference). That is, for the receiver to successfully decode the packet, the interference power at the AP should not exceed β.

B. OPTIMAL PCS THRESHOLD FOR SPATIAL REUSE

Constraints (15b) and (15c) are responsible for two phenomena inherent in the CSMA/CA protocol. First, is the *hidden terminal* problem, which occurs when the STA$_n$ senses no active transmission on the channel (i.e. $\mathbb{I}_c < \Upsilon$ is satisfied) but the interference power received at the AP hinders or is too high ($P_I > \beta$) for successful packet reception. The second problem is the *exposed terminal* problem, which results from STA$_n$ sensing a busy channel ($\mathbb{I}_c > \Upsilon$) but the interference power at the receiver AP does not affect packet reception ($P_I < \beta$). It is therefore possible that STA$_n$ will defer its transmissions even though the receiver AP could successfully decode its packets. Given the impacts of these events on the system throughput, our goal is to find Υ such that constraints (15b) and (15c) are satisfied, and achieve spatial reuse by mitigating the hidden terminal and the exposed terminal problems.

The interference power P_I in constraint (15c) can be expressed in terms of the SINR in Eqn. (2) satisfying the requirement, SINR$_n \geq \gamma$ as follows:

$$\begin{aligned} \text{Tr}\left(\mathbf{W}_n^H \mathbf{H}_n \mathbf{x}_n\right) \geq \underbrace{\mathbb{E}\left[\left|\sum_{\kappa \in \mathcal{K}, \kappa \neq n | \mathcal{K} \subset \mathcal{N}} \mathbf{W}_n \mathbf{H}_\kappa \mathbf{x}_\kappa\right|^2\right]\gamma}_{P_I} \\ + \mathbb{E}\left[|\mathbf{W}_n \mathbf{n}_o|^2\right]\gamma \quad \text{(16)} \end{aligned}$$

$$P_I \leq \text{Tr}\left(\mathbf{W}_n^H \mathbf{H}_n \mathbf{x}_n\right)\gamma^{-1} - \mathbb{E}\left[|\mathbf{W}_n \mathbf{n}_o|^2\right]. \quad \text{(17)}$$

Constraint (17) is derived from Eqn. (2) assuming that the SINR threshold γ accounts for the minimum tolerable interference power. In other words, Eqn. (17) establishes the minimum interference at which a node could decode packets successfully. Additionally, to guard against interference, P_I can be expressed in terms of the PCS threshold Υ as illustrated in Fig. 5. In this figure, STA 6 is located in the hidden terminal region and has the potential to interfere with the transmission of STA 3 at the AP. Since STA 6 is outside of the CSR χ of STA 3, STA 3 is completely unaware

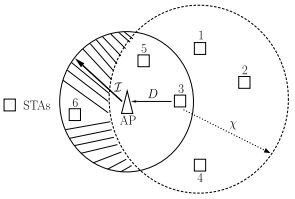

FIGURE 5. Relationships among carrier sensing range χ, interference range $\mathcal{I}$ and hidden terminal region [5].

of STA 6's transmission and a collision is bound to occur. To prevent the hidden terminal problem, the CSR χ should ideally cover the interference region $\mathcal{I}$ [5], i.e.,

$$\mathcal{I} \leq \chi + D, \quad \text{(18)}$$

and from this relationship, we can infer that in the worst case scenario $P_I = (\chi + D)^{-\alpha}$. Consequently, (17) can be written as:

$$\Upsilon \leq \text{Tr}\left(\mathbf{W}_n^H \mathbf{H}_n \mathbf{x}_n\right)\gamma^{-1} - \mathbb{E}\left[|\mathbf{W}_n \mathbf{n}_o|^2\right] - D^{-\alpha}. \quad \text{(19)}$$

By replacing (15c) with (19), (15) is equivalent to the following problem:

Lemma 3: The spatial density of throughput maximization problem in (15) becomes

$$\begin{aligned} &\text{maximize} && \mathcal{R}_{\text{SDT}} && \text{(20a)}\\ &\text{subject to} && \mathbb{I}_c \leq \Upsilon && \text{(20b)}\\ & && \Upsilon \leq \text{Tr}\left(\mathbf{W}_n^H \mathbf{H}_n \mathbf{x}_n\right)\gamma^{-1} - \Psi && \text{(20c)}\\ & && \Upsilon > 0, \quad \forall n \in \mathcal{N}, && \text{(20d)} \end{aligned}$$

where $\Psi = \mathbb{E}\left[|\mathbf{W}_n \mathbf{n}_o|^2\right] - D^{-\alpha}$. The solution to (20) depends on the selection of the PCS threshold to maximize the throughput density. Here, the Karush-Kuhn-Tucker (KKT) conditions are sufficient to find the optimal PCS threshold. From (13), (20) and Lemma 1, we can obtain a solution to this problem by formulating its Lagrange function

$$\begin{aligned} &\mathcal{L}(\Upsilon, \mu_1, \mu_2) \\ &= \lambda_n \mathcal{P}_n^\gamma - \lambda_n^2 \mathcal{P}_n^\gamma \Gamma\left(\frac{1}{\alpha}\right)\frac{1}{\alpha}\left(\frac{\Upsilon - \mathbb{E}\left[|\mathbf{W}_n \mathbf{n}_o|^2\right]}{\Theta_{\tilde{n}}}\right)^{-\frac{1}{\alpha}} \\ &\quad + \mu_1(\mathbb{I}_c - \Upsilon) + \mu_2\left(\text{Tr}\left(\mathbf{W}_n^H \mathbf{H}_n \mathbf{x}_n\right)\gamma^{-1} - \mathbb{E}\left[|\mathbf{W}_n \mathbf{n}_o|^2\right]\right. \\ &\quad \left. - D^{-\alpha} - \Upsilon\right) \quad \text{(21)} \end{aligned}$$

where μ_1 and μ_2 are Lagrange multipliers that penalize the violation of constraints (20b) and (20c), respectively. Obtaining the optimal $\hat{\mu}_1$ and $\hat{\mu}_2$ from (21) by satisfying KKT conditions [39], the optimal PCS threshold that maximizes the spatial density of throughput is obtained as

Theorem 1: The optimal PCS threshold $\hat{\Upsilon}$ that maximizes the spatial density throughput under the CSMA/CA

protocol is

$$\hat{\Upsilon} = \left[\left(\frac{\hat{\mu}_2 - \hat{\mu}_1}{\lambda_n^2 \frac{1}{\alpha} \Gamma\left(\frac{1}{\alpha}\right) \left(\frac{1}{\Theta_{\tilde{n}}}\right)^{-\frac{1}{\alpha}}} \right)^{-\frac{1-\alpha}{2\alpha}} \right]^+, \tag{22}$$

where $[\cdot]^+ \equiv \max\{\cdot, 0\}$.

Proof. Let $\hat{\mu}_1$ and $\hat{\mu}_2$ represent the optimal Lagrangian multiplier for constraints (20b) and (20c), respectively, and by taking the derivative of the Lagrangian function of (20) given in Equation (21) w.r.t Υ, we obtain the KKT conditions as follows:

$$\frac{\partial \mathcal{L}(\Upsilon, \mu_1, \mu_2)}{\partial \Upsilon} = 0, \hat{\mu}_1 \geq 0, \hat{\mu}_2 \geq 0, \\ \hat{\mu}_1 \hat{\Upsilon} - \hat{\mu}_1 \mathbb{I}_c = 0, \tag{23}$$

$$\mu_2 \Upsilon - \mu_2 \mathrm{Tr}\left(\mathbf{W}_n^H \mathbf{H}_n \mathbf{x}_n\right) \gamma^{-1} - \mu_2 D^{-\alpha} \\ + \mu_2 \left| U_r \sigma^2 \mathbf{I}_{U_r} \right|^2 = 0, \hat{\Upsilon} > 0, \tag{24}$$

and from (23), the following expression is obtained:

$$-\hat{\Upsilon}^{-\frac{1-\alpha}{\alpha}} \mathcal{P}_n^{\gamma} \lambda_n^2 \frac{1}{\alpha} \Gamma\left(\frac{1}{\alpha}\right) \left(\frac{1}{\Theta_{\tilde{n}}}\right)^{-\frac{1}{\alpha}} - \hat{\mu}_1 - \hat{\mu}_2 = 0, \tag{25}$$

where it is assumed that the noise term can be neglected during the PCS process. Since the selected PCS threshold value should generate low enough interference such that each node can achieve the desired data rate by satisfying the SINR threshold, setting $\mathcal{P}_n^{\gamma} = 1$ in (25), we have

$$\hat{\mu}_2 = \hat{\Upsilon}^{-\frac{1-\alpha}{\alpha}} \lambda_n^2 \frac{1}{\alpha} \Gamma\left(\frac{1}{\alpha}\right) \left(\frac{1}{\Theta_{\tilde{n}}}\right)^{-\frac{1}{\alpha}} + \hat{\mu}_1. \tag{26}$$

By substituting (26) into (24), the optimal PCS threshold to maximize the spatial density of throughput is obtained as:

$$\hat{\Upsilon} = \left[\left(\frac{\hat{\mu}_2 - \hat{\mu}_1}{\lambda_n^2 \frac{1}{\alpha} \Gamma\left(\frac{1}{\alpha}\right) \left(\frac{1}{\Theta_{\tilde{n}}}\right)^{-\frac{1}{\alpha}}} \right)^{-\frac{1-\alpha}{2\alpha}} \right]^+, \tag{27}$$

where $[\cdot]^+ = \max\{\cdot, 0\}$, which proves Equation (22). ■

Algorithm 1 Proposed PCS Threshold Selection

Input: α, λ_n, $\Theta_{\tilde{n}}$, γ
Output: PCS threshold $\hat{\Upsilon}$
Initialize μ_1, μ_2
$k = 1$ (*Number of iterations.*)
repeat
  Calculate $\hat{\Upsilon}$ using (27)
  Update $\hat{\mu}_1$ using (28)
  Update $\hat{\mu}_2$ using (29)
  $k \leftarrow k + 1$
until $\hat{\Upsilon}$ *converges*;
Set $\hat{\Upsilon}$ as PCS threshold for contention.

From Equation (22), we can infer that the PCS threshold selection that improves spatial reuse depends on network parameters, i.e., path loss, number of transmit antennas at the STAs, and the density of nodes. The Lagrange multipliers $\hat{\mu}_2$ and $\hat{\mu}_1$ can be obtained through line search such as the bisection method [39]. Algorithm 1 summarizes the steps in obtaining the optimal PCS threshold according to Theorem 1. Using subgradient updating, s^k represents the sequence of positive scalar step sizes [40] to update the Lagrangian multipliers μ_1 and μ_2 using Eqns. (28) and (29), respectively.

$$\mu_1^{k+1} = \left[\mu_1^k + s^k \left(\Upsilon - \mathbb{I}_c\right)\right]^+, \tag{28}$$

and

$$\mu_2^{k+1} = \left[\mu_2^k + s^k \left(\mathrm{Tr}\left(\mathbf{W}_n^H \mathbf{H}_n \mathbf{x}_n\right) \gamma^{-1} - \Psi - \Upsilon\right)\right]^+. \tag{29}$$

C. OPTIMAL NODE DENSITY AND THROUGHPUT

Under the PCS threshold selection framework assumed in Theorem 1, the optimal node density that can be supported to mitigate the effect of interference from a large number of concurrent transmitters can be derived from the mean rate given in (14) per unit bandwidth. By substituting Equation (22) into (14), we have:

$$\bar{\mathcal{R}} = \lambda_n \cdot \log\left(1+\gamma\right) \mathcal{P}_n^{\gamma} \left(1 - \left[\lambda_n \Gamma\left(\frac{1}{\alpha}\right) \left(\frac{\hat{\Upsilon}}{\Theta_{\tilde{n}}}\right)^{-\frac{1}{\alpha}} \frac{1}{\alpha}\right]\right)$$

$$= \lambda_n \log\left(1+\gamma\right) \mathcal{P}_n^{\gamma} - \lambda_n^{2(1-\alpha)} \mathcal{P}_n^{\gamma} \log\left(1+\gamma\right) \\ \left(\frac{\frac{1}{\alpha} \Gamma\left(\frac{1}{\alpha}\right) \left(\frac{1}{\Theta_{\tilde{n}}}\right)^{-\frac{1}{\alpha}}}{\hat{\mu}_2 - \hat{\mu}_1} \right)^{\frac{1-\alpha}{2}}, \tag{30}$$

and to evaluate the optimal node density that can be supported with SINR threshold γ, the mean rate can be optimized via:

$$\max_{\lambda_n} \bar{\mathcal{R}}. \tag{31}$$

The optimal node density is immediate from

Lemma 4: The optimal node density $\hat{\lambda}_n$ supported by the PCS threshold $\hat{\Upsilon}$ can expressed as

$$\hat{\lambda}_n = \left[\left(\frac{\frac{1}{\alpha} \Gamma\left(\frac{1}{\alpha}\right) \cdot \left(\frac{1}{\Theta_{\tilde{n}}}\right)^{-\frac{1}{\alpha}}}{\hat{\mu}_2 - \hat{\mu}_1} \right)^{\frac{1-\alpha}{2}} (2 - 2\alpha) \right]^{-\frac{1-2\alpha}{2}}. \tag{32}$$

Proof: The proof is obtained by setting the derivative of (30) with respect to λ_n equal to zero. ■

In (32), $\hat{\lambda}_n$ represents the maximum density of users allowed in the network for the PCS threshold $\hat{\Upsilon}$ to be effective in achieving the optimal target rate, resulting in

Theorem 2: An upper bound mean rate per Hz using the optimal density $\hat{\lambda}_n$ is

$$\bar{\mathcal{R}}\left(\hat{\lambda}_n\right) = \frac{\log\left(1+\gamma\right)}{\left[\left(\frac{\frac{1}{\alpha}\Gamma\left(\frac{1}{\alpha}\right)\cdot\left(\frac{1}{\Theta_{\tilde{n}}}\right)^{-\frac{1}{\alpha}}}{\hat{\mu}_2-\hat{\mu}_1}\right)^{\frac{1-\alpha}{2}}(2-2\alpha)\right]^{\frac{1-2\alpha}{2}}} \tag{33}$$

Proof: Substituting $\hat{\lambda}_n$ obtained from Lemma 4, $\mathcal{P}_n^c = 1$ and $\mathcal{P}_n^\gamma = 1$ in Equation (14), (33) is obtained. This implies that under the optimal node density $\hat{\lambda}_n$, the optimal mean rate is achievable when each node transmits with probability $\mathcal{P}_n^c = 1$ and achieves SINR above γ with probability $\mathcal{P}_n^\gamma = 1$, which is the ideal case. ■

V. SIMULATION AND PERFORMANCE ANALYSIS

A. SIMULATION SETUP

We assume a 2-D dense WLAN in a 800m×800m plane with varying STA density λ_n and AP density $\lambda_m = 0.2$ throughout the simulation, given different target SINR thresholds γ. The realizations of the PPPs with intensities λ_n and λ_m model STAs and APs locations, respectively, while the symbol energy $\mathcal{E}_x$ is normalized to unity. The path loss exponent $\alpha = 3.4$, which represents the ITU "rush-hour" propagation and $\sigma_{n_o}^2 = \frac{-100}{2}$ dBm. While the angle of arrival $\theta_{\tilde{n}} = \theta_\kappa = \frac{\pi}{2}$ throughout the simulation, the antenna spacing $\psi_y = 0.1 \cdot \omega$, where the wavelength ω corresponding to the 5 GHz band for WLAN. For most scenarios, the numbers of antennas at the APs are $K_r = \{1, 2, 4, 8\}$ while $U_r = U_t = 2$ for all STAs. Setting the PCS threshold according to Theorem 1, the spatial density of throughput and the mean rate are determined according to Eqns. (13) and (14), respectively. The evaluations of each node density λ_n is performed over 10^6 Monte Carlo realizations of the network to measure the density of successful transmissions.

For channel access control under the CSMA/CA protocol, the distributed coordinated function (DCF) is simulated for each of the PCS threshold schemes with a time-slot of $20\mu s$ and other MAC parameters as defined in the 802.11 standard. To determine which STAs are associated with a given AP, that is, belonging to the same BSS, we assume the legacy strongest signal first (SSF) association where STAs associate with their minimum distance AP. For performance benchmarking, the proposed scheme is compared with the legacy fixed PCS threshold selection and the DSC scheme. For the legacy scheme, the PCS threshold is fixed and identical for all nodes; it is set to -82 dBm [41] while the PCS threshold selection for the DSC scheme is [28]:

$$\Upsilon' = \min\left(\max\left(\Upsilon_{dsc}, \Upsilon_{\min}\right), \Upsilon_{\max}\right), \tag{34}$$

where, given the RSSI and a constant margin ξ , $\Upsilon_{dsc} = \text{RSSI (dBm)} - \xi$ (dB), $\Upsilon_{\min}$ and $\Upsilon_{\max}$ are the minimum and the maximum PCS threshold values allowed, respectively. The parameters for the DSC scheme are as follows: $\Upsilon_{\min} = -82$dBm, $\Upsilon_{\max} = -30$ dBm, and $\xi = 20$ dB. Basically, the system performance is assessed using the SDT and the mean rate using the proposed PCS threshold computation in Algorithm 1 versus the legacy global fixed and DSC schemes.

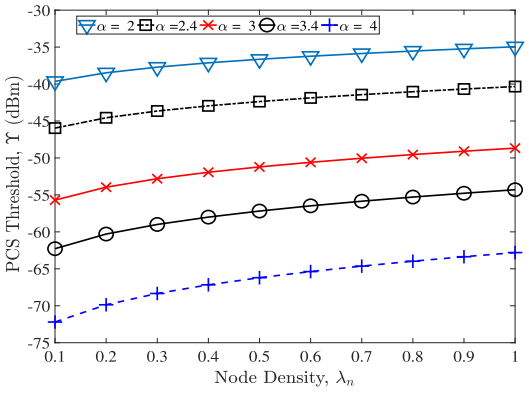

FIGURE 6. PCS Threshold Υ obtained from Eqn. (22) for various path loss exponents α as a function of node density λ_n.

B. SIMULATION RESULTS AND PERFORMANCE BENCHMARKING

First, the effectiveness of the proposed PCS threshold selection expressed in Theorem 1 is examined. In Fig. 6, for a given wireless environment, the proposed PCS threshold selection scheme adapts the PCS threshold value to specific node density λ_n and path loss exponent α. Observing node density $\lambda_n = 0.3$, the PCS threshold for $\alpha = 2$ is higher than that of $\alpha > 2$. As expected, the sensing range or CSR needs to be shorter in a low path loss environment. Also, as node density increases, regardless of the wireless environment, the PCS threshold needs to scale such that the contention domain or CSR of each node is more conservative. More specifically, higher PCS threshold permits more concurrent transmitters and implies strong interference. Low PCS threshold implies fewer concurrent transmitters and less interference. The proposed PCS threshold selection scheme finds a balance between these two extremes.

For different node densities the spatial density of throughput (SDT) is plotted in Fig. 7(a) for SINR threshold $\gamma = 5$ dB and $K_r = 8$ receiving antennas at the APs. The proposed PCS threshold selection scheme achieves a significant gain, above 60%, over the existing legacy system and the DSC scheme; this gain is not surprising as the PCS threshold is optimized for a specific node density rather than setting a globally fixed PCS threshold or performing an update based on some channel measurements. It is apparent that selecting a PCS threshold for each node density becomes more important as network density increases. Under the same parameters of $\gamma = 5$ dB and $K_r = 8$, Fig. 7(b) depicts the mean rate in nats/Hz/sec, which reveals the significant improved performance of the proposed scheme. As the node density increases, the mean rate under the legacy system and the DSC scheme decreases drastically while the proposed scheme achieves a rate that declines only modestly with increasing node density.

For SINR threshold $\gamma = -10$ dB, Fig. 8 depicts the achievable mean rate of the three schemes. The key

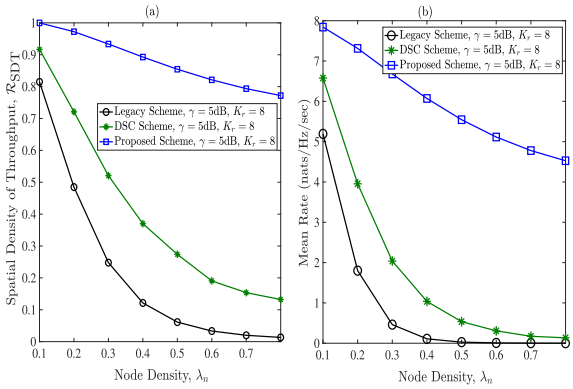

FIGURE 7. (a) Spatial density of throughput versus node density for $K_r = 8$ and $U_t = 2$. (b) Mean rate per node density at SINR $\gamma = 5$dB for $K_r = 8$ and $U_t = 2$.

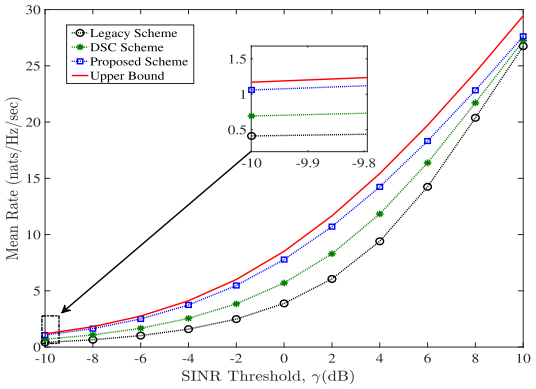

FIGURE 10. Comparing Mean Rate for $K_r = 8$ and $\lambda_n = 0.8$ to upper-bound rate (Theorem 2) for $K_r = 8$ and $\hat{\lambda}_n$.

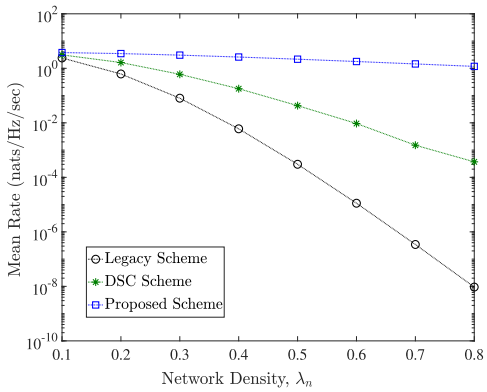

FIGURE 8. Mean Rate per Node Density λ_n given target SINR, $\gamma = -10$ (dB) for $K_r = 8$.

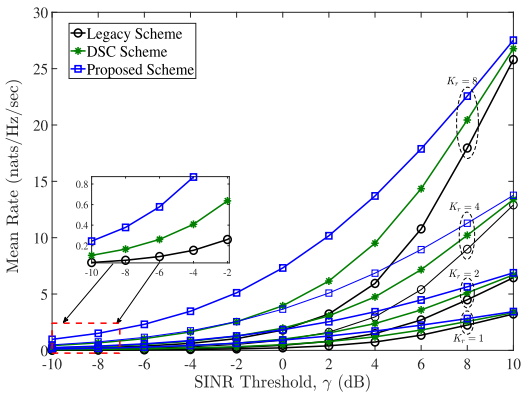

FIGURE 9. Mean Rate per target SINR, γ for various numbers of receive antennas K_r and given node density $\lambda_n = 0.8$.

observation in Fig. 8 is that performance improvement is obtained under the proposed scheme even at high node density. For various SINR thresholds, Fig. 9 depicts the mean rate of users achieving different SINRs with node density $\lambda_n = 0.8$. When the PCS threshold is obtained using the proposed scheme, a significant gain is achieved for each antenna array size K_r at the APs. This performance gain over the Legacy and the DSC schemes is due to the fact that adapting the PCS threshold to specific node density mitigates excessive interference from concurrent transmitters by allowing the appropriate number of nodes to transmit at each time slot. Fig. 10 compares the mean rate of the proposed PCS threshold, the DSC and the Legacy schemes to the upper bound rate defined in Theorem 2. At low SINR, for instance, $\gamma = -10$ dB, the proposed scheme achieves rate close to the upper bound obtained at the optimal node density $\hat{\lambda}_n$ from Lemma 4. Although at high SINR, the achievable rate of the proposed scheme slowly diverges away from the optimum value, it outperforms the DSC and the Legacy schemes.

VI. CONCLUSIONS

Selecting the PCS threshold value to improve spatial reuse in large-scale CSMA/CA WLAN remains challenging and is addressed in this paper, where it becomes imperative that PCS threshold design be network-specific; take several network parameters such as node density, antenna configuration, path loss and target rates into account. Without requiring the overhead of high rate channel parameter measurements, we derive a closed-form expression for selecting PCS threshold in CSMA/CA MIMO-WLANs assuming nodes that are randomly distributed according to PPP.

Rather than setting a default vendor-dependent value in hardware, our proposed framework selects PCS threshold for specific network types based on parameters such as path loss exponent and node density, which are global and obtainable during network planning. The proposed PCS threshold selection policy achieves target SINR (or rate) when other crucial network parameters are known a priori and improves the spatial density of throughput over the legacy globally fixed PCS threshold and the dynamic sensitivity control (DSC) schemes when tested in a simulated MIMO-WLAN based on the DCF CSMA/CA protocol. The advantage of optimizing the PCS threshold is that this important network parameter scales with the node density and is selected for specific wireless network environment; thereby improving overall system performance.

APPENDIX A
PROOF OF LEMMA 2

To prove Equation (12) in Lemma 2 from Eqn. (2), the probability

$$
\begin{aligned}
&\mathbb{P}\left[\mathrm{SINR}_n > \gamma\right] \\
&= \left|\mathbf{W}_n^H \Theta_n \mathbf{R}_n \mathbf{W}_n\right|^2 \\
&> \gamma \left(\left| \sum_{\kappa\in\mathcal{K},\kappa\neq n|\mathcal{K}\subset\mathcal{N}} \mathbf{W}_n^H \left(\mathbf{R}_\kappa \Theta_\kappa + \mathbb{E}\left[\mathbf{n}_o \mathbf{n}_o^H\right]\right) \mathbf{W}_n \right|^2 \right) \\
&\overset{(a)}{=} \left|\mathbf{W}_n^H \Theta_n \mathbf{R}_n \mathbf{W}_n\right|^2 \\
&> \left| \gamma \left(\sum_{\kappa\in\mathcal{K},\kappa\neq n|\mathcal{K}\subset\mathcal{N}} \mathbf{W}_n^H \left(\mathbf{R}_\kappa \Theta_\kappa + \mathbb{E}\left[\mathbf{n}_o \mathbf{n}_o^H\right]\right) \mathbf{W}_n \right) \right|^2 \\
&= \left|\mathbf{W}_n^H \Theta_n \mathbf{R}_n \mathbf{W}_n\right|^2 > \left| \mathbf{W}_n^H \left(\sum_{\kappa\in\mathcal{K},\kappa\neq n|\mathcal{K}\subset\mathcal{N}} \gamma \mathbf{R}_\kappa \Theta_\kappa \right) \mathbf{W}_n \right|^2 \\
&\quad + \gamma \mathbb{E}\left[\mathbf{n}_o \mathbf{n}_o^H\right] \left\| \mathbf{W}_n^H \right\| \\
&\overset{(b)}{\geq} \mathbb{E}\left[\exp\left(-\gamma \left\|\mathbf{W}_n\right\|^2 \left| K_r \sigma_{n_o}^2 \mathbf{I}_{K_r} \right|^2 \right) \right. \\
&\quad \left. \exp\left(-\gamma \left| \mathbf{W}_n^H \underbrace{\left(\sum_{\kappa\in\mathcal{K},\kappa\neq n|\mathcal{K}\subset\mathcal{N}} \left| e^{j2\theta_\kappa} U_t \mathcal{E}_x \mathbf{I}_{U_t} \right|^2 \mathbf{R}_\kappa \right)}_{P_I} \mathbf{W}_n \right|^2 \right) \right] \\
&\overset{(c)}{=} \exp\left(-\gamma \left\|\mathbf{W}_n\right\|^2 \left| K_r \sigma_{n_o}^2 \mathbf{I}_{K_r} \right|^2 \right) \cdot \\
&\quad \mathbb{E}_{P_I}\left[e^{-\gamma \left| \mathbf{W}_n^H \left(\sum_{\kappa\in\mathcal{K},\kappa\neq n|\mathcal{K}\subset\mathcal{N}} \left| e^{j2\theta_\kappa} U_t \mathcal{E}_x \mathbf{I}_{U_t} \right|^2 \mathbf{R}_\kappa \right) \mathbf{W}_n \right|^2 } \right] \\
&\overset{(d)}{=} \exp\left(-\gamma \left\|\mathbf{W}_n\right\|^2 \left| K_r \sigma_{n_o}^2 \mathbf{I}_{K_r} \right|^2 \right) \\
&\quad \exp\left(-\gamma \left| \mathbf{W}_n^H \left(\sum_{\kappa\in\mathcal{K},\kappa\neq n|\mathcal{K}\subset\mathcal{N}} \left| e^{j2\theta_\kappa} U_t \mathcal{E}_x \mathbf{I}_{U_t} \right|^2 \mathbf{R}_\kappa \right) \mathbf{W}_n \right|^2 \right) \\
&\overset{(e)}{=} \Psi \exp\left(-\gamma \left| \mathbf{W}_n^H \left(\left| e^{j2\theta_\kappa} U_t \mathcal{E}_x \mathbf{I}_{U_t} \right|^2 \right. \right. \right. \\
&\quad \left. \left. \left. \mathbb{E}_{\kappa\in\mathcal{N}\setminus n} \left[\sum_{\kappa\in\mathcal{K},\kappa\neq n|\mathcal{K}\subset\mathcal{N}} \mathbf{R}_\kappa \right] \right) \mathbf{W}_n \right|^2 \right) \qquad (35)
\end{aligned}
$$

where $\Psi = \exp\left(-\gamma \left\|\mathbf{W}_n\right\|^2 \left| K_r \sigma_{n_o}^2 \mathbf{I}_{K_r} \right|^2 \right)$, (a) follows from substituting Eqn. (4) into (35), (b) is obtained from the exponential property of the CSI, (c) follows from the fact that (b) is an expectation of the interference power P_I received from other concurrently transmitting STAs. The expectation of the interference power w.r.t to each interference channel $\mathbf{H}_\kappa$ of source κ is captured in (d) where $\mathbf{R}_\kappa = \mathbb{E}\left[\mathbf{H}_\kappa \mathbf{H}_\kappa^H\right]$ is given by Eqn. (7). Then (e) is an expectation of interference power over the set $\mathcal{K}$ of stochastic interference points. By substituting $\mathbf{R}_\kappa$ in (e) using Eqn. (7), we have

$$
\begin{aligned}
&\overset{(f)}{=} \Psi \exp\left(-\gamma \left| \mathbf{W}_n^H \left(\left| e^{j2\theta_\kappa} U_t \mathcal{E}_x \mathbf{I}_{U_t} \right|^2 \right. \right. \right. \\
&\quad \left. \left. \left. \mathbb{E}_{\kappa\in\mathcal{N}\setminus n} \left[\sum_{\kappa\in\mathcal{K},\kappa\neq n|\mathcal{K}\subset\mathcal{N}} J_0\left(\Delta\psi_y \frac{2\pi}{\omega} \right) \right] \right) \mathbf{W}_n \right|^2 \right) \\
&\overset{(g)}{=} \Psi \exp\left(-\gamma \left| \mathbf{W}_n^H \left(\left| e^{j2\theta_\kappa} U_t \mathcal{E}_x \mathbf{I}_{U_t} \right|^2 \lambda_n \right. \right. \right. \\
&\quad \left. \left. \left. \int_0^\infty J_0\left(\Delta\psi_y \frac{2\pi}{\omega} \right) \right) \mathbf{W}_n \right|^2 \right)
\end{aligned}
$$

where (g) is obtained by applying *Slivnyak-Mecke*'s theorem, $\mathbb{E}\sum_{x\in\Phi} f(x, \Phi\setminus x) = \lambda \int_{\mathbb{R}^d} \mathbb{E} f(x, \Phi)\, dx$ [11], [37]. By simplifying the $\int_0^\infty J_0(\cdot)$ term using the integral transformation [36, Eqn. 6.554.1], (g) evaluates to the closed-form expression, Eqn. (12). ■

REFERENCES

[1] C. Thorpe and L. Murphy, "A survey of adaptive carrier sensing mechanisms for IEEE 802.11 wireless networks," *IEEE Commun. Surveys Tuts.*, vol. 16, no. 3, pp. 1266–1293, 3rd Quart., 2014.

[2] L. Ho and H. Gacanin, "Design principles for ultra-dense Wi-Fi deployments," in *Proc. IEEE WCNC*, Apr. 2018, pp. 1–6.

[3] Z. Zhong, F. Cao, P. Kulkarni, and Z. Fan, "Promise and perils of dynamic sensitivity control in IEEE 802.11ax WLANs," in *Proc. Int. Symp. Wireless Commun. Syst.*, Poznan, Poland, Sep. 2016, pp. 20–23.

[4] P. Kulkarni and F. Cao, "Taming the densification challenge in next generation wireless LANs: An investigation into the use of dynamic sensitivity control," in *Proc. IEEE 11th WiMob*, Oct. 2015, pp. 860–867.

[5] Y. Zhu, Q. Zhang, Z. Niu, and J. Zhu, "On optimal QoS-aware physical carrier sensing for IEEE 802.11 based WLANs: Theoretical analysis and protocol design," *IEEE Trans. Wireless Commun.*, vol. 7, no. 4, pp. 1369–1378, Apr. 2008.

[6] A. M. Voicu, F. Giorgi, L. Simic, and M. Petrova, "Wi-Fi evolution for future dense networks: Does sensing threshold adaptation help?" in *Proc. IEEE WCNC*, Barcelona, Spain, Apr. 2018, pp. 1–6.

[7] A. Valkanis, A. Iossifides, P. Chatzimisios, M. Angelopoulos, and V. Katos, "IEEE 802.11ax spatial reuse improvement: An interference-based channel-access algorithm," *IEEE Veh. Technol. Mag.*, vol. 14, no. 2, pp. 78–84, Jun. 2019.

[8] Y. Kim, F. Baccelli, and G. de Veciana, "Spatial reuse and fairness of ad hoc networks with channel-aware CSMA protocols," *IEEE Trans. Inf. Theory*, vol. 60, no. 7, pp. 4139–4157, Jul. 2014.

[9] T. V. Nguyen and F. Baccelli, "On the spatial modeling of wireless networks by random packing models," in *Proc. IEEE INFOCOM*, Mar. 2012, pp. 28–36.

[10] Y. Li, F. Baccelli, J. G. Andrews, T. D. Novlan, and J. C. Zhang, "Modeling and analyzing the coexistence of Wi-Fi and LTE in unlicensed spectrum," *IEEE Trans. Wireless Commun.*, vol. 15, no. 9, pp. 6310–6323, Sep. 2016.

[11] M. Haenggi and R. K. Ganti, "Interference in large wireless networks," *Found. Trends Netw.*, vol. 3, no. 2, pp. 127–248, 2009.

[12] P. B. Oni and S. D. Blostein, "Optimized physical carrier sensing threshold in high density CSMA/CA networks," in *Proc. IEEE 29th Biennial Symp. Commun.*, Toronto, ON, Canada, Jun. 2018, pp. 1–5.

[13] I. Jamil, L. Cariou, and J.-F. Helard, "Improving the capacity of future IEEE 802.11 high efficiency WLANs," in *Proc. 21st IEEE Int. Conf. Telecommun.*, Lisbon, Portugal, May 2014, pp. 303–307.

[14] Y. Li, J. Zheng, and Q. Li, "Enhanced listen-before-talk scheme for frequency reuse of licensed-assisted access using LTE," in *Proc. PIMRC*, Aug./Sep. 2015, pp. 1918–1923.

[15] K. T. Phan, J. Park, M. van der Schaar, "Near-optimal deviation-proof medium access control designs in wireless networks," *IEEE/ACM Trans. Netw.*, vol. 20, no. 5, pp. 1581–1594, Oct. 2012.

[16] Y.-S. Liou, R.-H. Gau, and C.-J. Chang, "Dynamically tuning aggression levels for capacity-region-aware medium access control in wireless networks," *IEEE Trans. Wireless Commun.*, vol. 13, no. 4, pp. 1766–1778, Apr. 2014.
[17] Y. Kim, M.-S. Kim, S. Lee, D. Griffith, and N. Golmie, "AP selection algorithm with adaptive CCAT for dense wireless networks," in *Proc. IEEE WCNC*, Mar. 2017, pp. 1–6.
[18] I. Jamil, L. Cariou, and J.-F. Hélard, "Carrier sensing-aware rate control mechanism for future efficient WLANs," in *Proc. Int. Conf. Workshop Netw. Future*, Dec. 2014, pp. 1–6.
[19] I. Roslan, T. Kawasaki, T. Nishiue, Y. Takaki, C. Ohta, and H. Tamaki, "Control of transmission power and carrier sense threshold to enhance throughput and fairness for dense WLANs," in *Proc. 30th ICOIN*, Jan. 2016, pp. 51–56.
[20] Y. Wen, H. Fujita, and D. Kimura, "Throughput-aware dynamic sensitivity control algorithm for next generation WLAN system," in *Proc. PIRMC*, Oct. 2017, pp. 1–7.
[21] M. S. Afaqui, E. Garcia-Villegas, E. Lopez-Aguilera, G. Smith, and D. Camps, "Evaluation of dynamic sensitivity control algorithm for IEEE 802.11ax," in *Proc. IEEE WCNC*, Mar. 2015, pp. 1060–1065.
[22] M. S. Afaqui, E. Garcia-Villegas, E. Lopez-Aguilera, and D. Camps-Mur, "Dynamic sensitivity control of access points for IEEE 802.11ax," in *Proc. IEEE ICC*, May 2016, pp. 1–7.
[23] S. Yoo, S. Kim, J. Yi, Y. Son, and S. Choi, "ProCCA: Protective clear channel assessment in IEEE 802.11 WLANs," *IEEE Commun. Lett.*, vol. 20, no. 5, pp. 958–961, May 2016.
[24] S. Kim, S. Yoo, J. Yi, Y. Son, and S. Choi, "FACT: Fine-grained adaptation of carrier sense threshold in IEEE 802.11 WLANs," *IEEE Trans. Veh. Technol.*, vol. 66, no. 2, pp. 1886–1891, May 2017.
[25] P. Kulkarni and F. Cao, "Dynamic sensitivity control to improve spatial reuse in dense wireless LANs," in *Proc. MSWiM*, 2016, pp. 323–329.
[26] I. Selinis, M. Filo, S. Vahid, J. Rodriguez, and R. Tafazolli, "Evaluation of the DSC algorithm and the BSS color scheme in dense cellular-like IEEE 802.11ax deployments," in *Proc. PIMRC*, Sep. 2016, pp. 1–7.
[27] Z. Zhang, Y. Li, K. Huang, and C. Liang, "On stochastic geometry modeling of WLAN capacity with dynamic sensitive control," in *Proc. 13th Int. Symp. Modeling Optim. Mobile, Ad Hoc, Wireless Netw. (WiOpt)*, May 2015, pp. 78–83.
[28] Z. Zhong and F. Cao, "Stochastic analysis of 802.11 uplink with dynamic sensitivity control," in *Proc. IEEE GLOBECOM*, Dec. 2016, pp. 1–6.
[29] Z. Ding, S. Xing, F. Yan, S. Deng, and L. Shen, "Correlation analysis and adaptive carrier sensing adjustment in dense random wireless networks," in *Proc. 9th Wireless Commun. Signal Process. (WCSP)*, Nanjing, China, Oct. 2017, pp. 1–6.
[30] Z. Ding, S. Xing, F. Yan, Z. Li, and L. Shen, "Impact of adaptive carrier-sensing range on the performance of dense wireless networks," in *Proc. 9th Wireless Commun. Signal Process. (WCSP)*, Nanjing, China, Oct. 2017, pp. 1–6.
[31] A. Aijaz and P. Kulkarni, "On performance evaluation of dynamic sensitivity control techniques in next-generation WLANs," *IEEE Syst. J.*, vol. 13, no. 2, pp. 1324–1327, Jun. 2019.
[32] Y. Zhang, B. Li, M. Yang, Z. Yan, and X. Zuo, "Joint optimization of carrier sensing threshold and transmission rate in wireless ad hoc networks," in *Proc. IEEE QSHINE*, Aug. 2015, pp. 210–215.
[33] K.-J. Park, J. Choi, J. C. Hou, Y.-C. Hu, and H. Lim, "Optimal physical carrier sense in wireless networks," *Ad Hoc Netw.*, vol. 9, no. 1, pp. 16–27, Jan. 2011.
[34] C.-K. Chau, I. W. H. Ho, Z. Situ, S. C. Liew, and J. Zhang, "Effective static and adaptive carrier sensing for dense wireless CSMA networks," *IEEE Trans. Mobile Comput.*, vol. 16, no. 2, pp. 355–366, Feb. 2017.
[35] H. Q. Nguyen, F. Baccelli, and D. Kofman, "A stochastic geometry analysis of dense IEEE 802.11 networks," in *Proc. IEEE INFOCOM*, Barcelona, Spain, May 2007, pp. 1199–1207.
[36] I. S. Gradshteyn and I. M. Ryzhik, *Table of Integrals, Series, and Products*. 7th ed. Amsterdam, The Netherlands: Elsevier, 2007.
[37] S. N. Chiu, D. Stoyan, W. S. Kendall, and J. Mecke, *Stochastic Geometry and Its Applications*, 3rd ed. Hoboken, NJ, USA: Wiley, 2013.
[38] D.-S. Shiu, G. J. Foschini, M. J. Gans, and J. M. Kahn, "Fading correlation and its effect on the capacity of multielement antenna systems," *IEEE Trans. Commun.*, vol. 48, no. 3, pp. 502–513, Mar. 2000.
[39] S. Boyd and L. Vandenberghe, *Convex Optimization*. Cambridge, U.K.: Cambridge Univ. Press, 2004.
[40] W. Yu and R. Lui, "Dual methods for nonconvex spectrum optimization of multicarrier systems," *IEEE Trans. Commun.*, vol. 54, no. 7, pp. 1310–1322, Jul. 2006.
[41] G. Smith, "Dynamic sensitivity control v2," DSP Group, San Jose, CA, USA, Tech. Rep. IEEE 802.11-13/1012r4, Nov. 2013. [Online]. Available: https://mentor.ieee.org/802.11/dcn/13/11-13-1012-04-0wng-dynamic-sensitivity-control.pptx

PHILLIP B. ONI (S'10) received the B.Sc. degree in telecommunications and wireless technologies from the American University of Nigeria, Nigeria, in 2010, and the M.Sc. and M.A.Sc. degrees in telecommunications engineering and electrical/computer engineering from University of Vaasa, Finland, and Queen's University, Canada, in 2013 and 2015, respectively, where he is currently pursuing the Ph.D. degree in electrical/computer engineering. His current research interest includes the application of graph theories and stochastic geometry in wireless communications with specific applications in analyzing and improving performance of high-density wireless networks (dense deployments) in unlicensed spectrum. He has served as a reviewer for IEEE Access, IEEE Transactions on Vehicular Technology, IEEE ICC, IEEE GLOBECOM, IEEE LNC, and IEEE SPAWC.

STEVEN D. BLOSTEIN (S'82–M'88–SM'96) received the B.S. degree in electrical engineering from Cornell University, Ithaca, NY, USA, in 1983, and the M.S. and Ph.D. degrees in electrical and computer engineering from the University of Illinois, Urbana–Champaign, IL, USA, in 1985 and 1988, respectively. From 2004 to 2009, he was the Department Head. Since 1988, he has been with the faculty of the Department of Electrical and Computer Engineering, Queen's University, Kingston, ON, Canada, where he is currently a Professor. He is a registered Professional Engineer in Ontario. He has also been a consultant to industry and government in the areas of image compression, target tracking, radar imaging, and wireless communications. His current interests include wireless communications systems, including detection and estimation, signal processing, energy efficiency, MIMO, dynamic access, and dense deployments.

Dr. Blostein was the Chair of the IEEE Kingston Section, the Chair of the Biennial Symposium on Communications, the Publications Chair IEEE ICASSP, an Associate Editor of the IEEE Transactions on Image Processing and the IEEE Transactions on Wireless Communications, and served on numerous Technical Program Committees for the IEEE Communications Society conferences.